J Solid State Electrochem (2007) 11:859–866
DOI 10.1007/s10008-006-0233-9

ORIGINAL PAPER

P and n dopable semi-interpenetrating polymer networks

T.-X. Lav · F. Tran-Van · J.-P. Bonnet · C. Chevrot · S. Peralta · D. Teyssié · J. V. Grazulevicius

Received: 21 July 2006 / Revised: 8 September 2006 / Accepted: 13 October 2006 / Published online: 1 December 2006

Abstract Electrochemical oxidation of thin films of 9-(2,3-epoxypropyl)carbazole (OEPC) oligomer deposited on an electrode leads to the formation of an in-situ cross-linked structure with biscarbazyl redox sites due to the anodic coupling of pendant carbazole units. Electrochemical, optical, and thermal characterizations confirm the formation of a conducting network containing electroactive biscarbazolyl units. When the electrochemical cross-linking takes place in a starting thin film containing a mixture of OEPC and a perylene bisimide polymer [poly(Pery-EO_3)], a semi-interpenetrating polymer network is formed which possesses both electron donor and electron acceptor properties. Indeed, the electrochemical behavior of the semi-interpenetrating polymers network (IPN) is characterized by two reversible oxidations and two reversible reduction waves corresponding to the biscarbazolyl and perylene redox moities, respectively. The energy levels of the highest occupied molecular orbital E_{HOMO} and lowest unoccupied molecular orbital E_{LUMO} of each donor and acceptor in the semi-IPN have been evaluated and indicate a possible electron transfer from biscarbazole to perylene, which could be taken advantage of in the field of solar cells application.

T.-X. Lav · F. Tran-Van · J.-P. Bonnet · C. Chevrot (✉) · S. Peralta · D. Teyssié
Laboratoire de Physico-Chimie des Polymères et des Interfaces,
Université de Cergy-Pontoise,
5 mail Gay-Lussac,
95031 Cergy-Pontoise Cedex, France
e-mail: Claude.Chevrot@chim.u-cergy.fr

J. V. Grazulevicius
Department of Organic Technology,
Kaunas University of Technology,
Radvilenu Plentas 19,
3028 Kaunas, Lithuania

Introduction

Organic solar cells have attracted much interest motivated by developing inexpensive, efficient, and renewable energy sources [1–4]. A highly promising route in this field concerns bulk heterojunction structures in which an electron donor and an electron acceptor are associated in a unique thin layer with the aim of obtaining a large-area donor–acceptor interface which will improve the exciton separation [5].

A lot of studies have been carried out on the association of an electron donor conjugated polymer such as polyparaphenylenevinylene or polyalkylthiophene derivative and an electron acceptor material, among which are fullerene derivatives [6–8], perylene derivatives [9–15], n dopable polymer [16, 17], or others [18, 19] in order to increase the dissociation efficiency. Among these electron-acceptors, perylene derivatives have received considerable attention due to their unique combination of optical, redox, and stability properties. Their electron-transport properties have also been reported in amorphous polymeric structures [20–22] or in self-organized architecture such as smectic discotic liquid crystal phases [23]. On the other hand, carbazole derivatives and, more particularly, poly(vinylcarbazole) have attracted attention in the field of photovoltaic devices due to their good photoconduction properties [24, 25]. Associations of carbazole and perylene derivatives in a mixture have already been examined [26–28]. Chen et al. [27] have studied a fluorinated perylene diimide doped polyvinyl carbazole film and shown high exciton dissociation and good electron transport ability. Müllen et al. [28] have designed a donor/acceptor pair composed of poly(2,7-carbazole) derivatives and perylene tetracarboxydiimide in bulk-heterojunction leading to a power efficiency of 0.6% under AM1.5 illumination.

In this paper, we have considered the design of a single layer two-component system through the combination of p and n dopable polymers into a semi-interpenetrating polymers network architecture (semi-IPNs). We have chosen an ethyleneoxide/carbazole based oligomer [oligoepoxypropylcarbazole (OEPC)] [29] as hole transporting material. The realization of the three-dimensional networks has been achieved by anodic coupling of carbazole pendant units in the presence of a polyimide [poly(Pery-EO_n)] containing electron-transporting perylenediimine moieties. The ethyleneoxyde units present in both materials are expected to ensure a good compatibility and, therefore, to limit the phase separation of the initial mixture deposited on the anode. Figure 1 shows a schematic representation of the blend before electrochemical oxidation and the formation of the semi-IPN after cross-linking of the pendant carbazole units.

First, the possibility to electrochemically cross-link a thin OEPC film will be presented. Then, it will be shown that the association of OEPC with the perylene bisimide-based polymer during the electrochemical oxidation leads to the formation of a p/n dopable semi-IPN. Extraction experiments of the linear polyimide from the semi-IPN during the electrochemical cross-linking process will be presented as an indirect kinetics witnessing the gradual formation of the semi-IPN. Energetic levels of biscarbazole and perylene bisimide units will be derived from electrochemical and optical characterizations. Finally, fluorescence quenching studies of perylene moieties in the polyimide in the presence of carbazole monomer will illustrate the possible electron transfer between the donor and the acceptor materials.

Experimental section

Reagent

Perylene-3,4,9,10-tetracarboxylic dianhydride, 4,7,10-trioxa-1,13-tridecanediamine, 1,4-butanesultone, and poly(ethylene glycol) bis (3-aminopropyl)terminated (1,500 g mol^{-1}) purchased from Aldrich were used without any treatment. *N*,*N*-dimethylformamide (DMF) purchased from Adrich was dried on calcium hydride and distilled under vacuum prior to use. Acetonitrile (VWR Prolabo), tetrabultylamonium perchlorate (Fluka), were used without further purification.

Synthesis of oligomer and polymer

Poly(Pery-EO_3) and poly(Pery-EO_{34}) (Fig. 2) were synthesized following the procedure previously described [30, 31]. The carbazole oligomer (OEPC) was synthesized by cationic polymerization of oxirane carbazole derivative using triphenylmethane cation salt as previously described [32].

4-carbazol-9-yl-butane-1-sulfonate sodium salt ($CzSO_3Na$) was synthesized by reaction of carbazole with sodium hydride in toluene, subsequent addition of butane sultone, and refluxing 6 h under stirring according to the method of Reynolds et al. [33]. Steric exclusion chromatography analysis of OEPC [using tetrahydrofurane (THF) as eluent and monodisperse polystyrene standards for the molecular weight evaluation] gives a molecular weight of M_n=650 with polydispersity index I_p=1.2 and an average polymerization degree of 2.9.

Apparatus

Cyclic voltammetries were performed with an Autolab Potentiostat/Galvanostat PGSTAT30 in a three-electrode single-compartment cell. The working electrode was either a platinum disc of 0.785 cm^2 or a glass substrate-coated indium tin oxide (ITO) electrode of 1.2 cm^2 (from Delta Technologies). The counter electrode consisted of a platinum wire and the reference electrode was a saturated calomel electrode. All potentials were internally referenced to the ferrocene–ferricinium couple. For the electrochemical synthesis of the semi-IPN, a mixture of OEPC and poly(Pery-EO_3) (1/1 wt.%) was dissolved in dichloromethane (2 mg/ml) before coating onto working electrode (20 µl), then evaporated. Electrochemical characterizations of the semi-IPN were carried out under saturated argon atmosphere after the solution was purged for 15 min.

UV-Vis and fluorescence spectra were recorded on a JASCO V570 and JASCO FP-6200 spectrometer either in

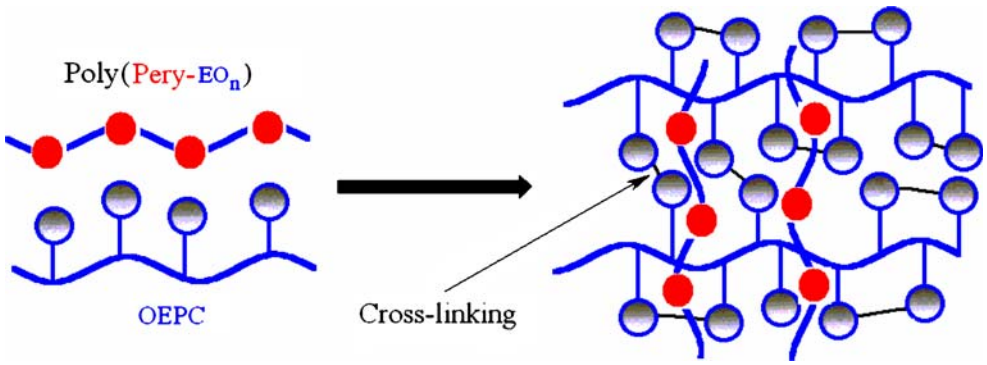

Fig. 1 Scheme of the electrochemical cross-linking

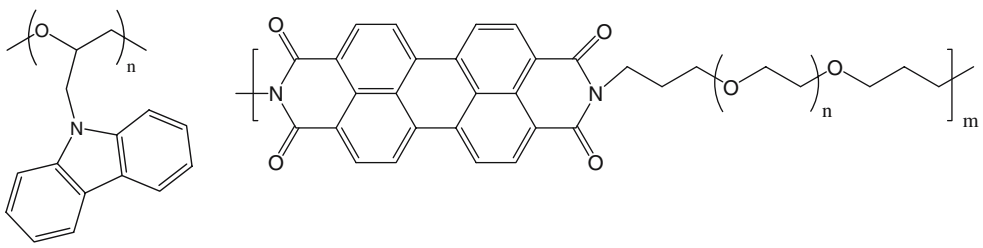

Fig. 2 **a** Chemical structure of OEPC oligomer and **b** poly (Pery-EO_n) polymers

OEPC **n= 2 : poly(Pery-EO_3)** **n=33 : poly(Pery-EO_{34})**

THF solution (in 5 mm length Q quartz cells) or on ITO substrate for solid state thin film before and after electrochemical cross-linking. Infrared spectra were performed with a Fourier transform infrared (FTIR) Tensor 27 BRÜKER spectrometer equipped with an attenuated total reflectance probe.

Morphological observations of specimens were carried out with a Dimension 3100 atomic force microscope (AFM) with a Nanoscope IIIa controller from Veeco Instruments. The images were acquired using intermittent contact mode under ambient conditions. The cantilevers used (Budget-Sensors) had nominal spring constants of 20–80 N/m and resonant frequencies in the range 200–260 kHz.

Thin films for AFM studies were prepared using a spin coater P6700 from Specialty Coating Systems. A solution of OEPC in dichloromethane (25 mg/ml) was spin-coated onto ITO substrates at 1,500 t/min.

Results and discussion

Synthesis, optical, and electrochemical characterization of poly(Pery-EO_n)

Polyimides containing perylene and oligoethyleneoxide moieties have been synthetized by polycondensation reaction between perylene-3,4,9,10-tetracarboxylic dianhydride and the corresponding diaminated oligoethers 4,7,10-trioxa-1,13-tridecanediamine or poly(ethylene glycol) bis(3-aminopropyl)terminated (1,500 g mol^{-1}) in refluxing DMF. The formation of imide linkage proceeds in two steps via a polyamic intermediate [30, 31]. Polyimides have been characterized by FTIR. The dianhydride C=O vibration bands (at 1,768, 1,753, 1,742, and 1,729 cm^{-1}) characteristic of the perylene starting monomer disappears after 20 h reaction and the concomitant appearance of imide C=O stretching vibration bands (at 1,692 and 1,655 cm^{-1}) confirms the completion of the condensation reaction [34, 35].

UV-visible and fluorescence spectroscopies were used to confirm the presence of the chromophore perylene units. Due to the number of ethylene oxide units, poly(Pery-EO_{34}) is quite soluble in common organic solvent by contrast with poly(Pery-EO_3). Thus, poly(Pery-EO_{34}) is preferred in this work for optical and electrochemical characterization, as well as fluorescence quenching (§d) studies, whereas poly (Pery-EO_3) will be chosen for the synthesis of the semi-IPN since it is insoluble in the electrolyte.

UV-visible spectra of a solution of poly(Pery-EO_{34}) in THF (at 0.7 g l^{-1}) shows two major peaks at 486 and 520 nm with shoulders at 457 and 426 nm, typical of a vibronic feature and corresponding to the electronic absorption from v=0 to v'=0,1,2,3 (where v and v' are quantum vibrational numbers of the ground and excited state, respectively) [36]. Fluorescence characterization of poly(Pery-EO_{34}) solutions as a function of concentration show a red shift of the emission band typical of the self association of the polyimide due to perylene π–π stacking. The nonaggregated free polymer chains (5.3 mg l^{-1}) emit at 524 nm (green), whereas a main emission band appears at 572 nm for a higher concentration solution (1.36 g l^{-1}), as already observed [35].

The electrochemical behavior of poly(Pery-EO_{34}) has been studied by cyclic voltammetry in solution of 0.1 M NBu_4ClO_4 in CH_3CN. Two reversible reduction waves are observed at half-wave potentials of, respectively, −1.11 and −1.21 V vs Fc/Fc^+, corresponding to the successive formation of anion and dianion radicals of redox perylene units [37, 38].

Electrochemical cross-linking of OEPC

In order to characterize the electrochemical behavior of OEPC, the oligomer was first deposited onto a platinum electrode (Pt) from a dichloromethane solution (by evaporation), and the modified electrode was subsequently immersed in 0.1 M $LiClO_4$ in CH_3CN. During the first anodic scan, the appearance of an oxidative current is observed for which the onset starts at 0.65 V vs Fc/Fc^+ and the oxidation peak current is reached at 0.95 V vs Fc/Fc^+ (Fig. 3). Such a curve is typical of the oxidation of carbazole derivatives, as already described for different substituted carbazoles monomers in solution [39, 40]. In the present work, the oligomer is deposited on the electrode and the oxidation process needs concomitant incorporation of anions in the bulk of the thin film to ensure the

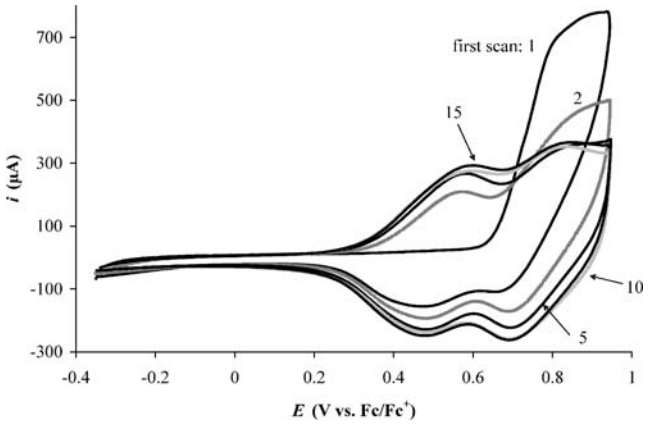

Fig. 3 Electrochemical cross-linking by cycling voltammetry (15 cycles) of thin film of OEPC onto Pt in $CH_3CN/LiClO_4$ (0.1 mol l^{-1}), v=50 mV s^{-1}

electroneutrality. Due to the presence of oligoethyleneoxide units, which are well known to favor ionic conductivity [41], the incorporation of ions is easy and the electroactivity of the carbazole redox units in the solid state is kept.

During the first reverse scan, it is already possible to observe two reduction peaks at 0.48 and 0.66 V vs Fc/Fc^+, which are characteristic of two new redox systems. During repeated scans, the intensity of the two redox systems grows up and reaches a maximum after 15 scans. These two reversible well defined oxidation peaks occur, respectively, at half-wave potentials of 0.54 and 0.77 V vs Fc/Fc^+. Such a general trend of OEPC cyclic voltammetry is similar to the one described by Ambrose et al. [39, 40] during the electrochemical oxidation of different N-substituted carbazole in solution leading to the formation of the corresponding dimer.

According to Ambrose [40], the first anodic peak can be assigned to the formation of the radical-cation and the second one to the formation of the dication of a carbazolic diade. The proposed mechanism of the formation of the biscarbazole network is described in Fig. 4.

In order to confirm the cross-linking, the solubility change of the film after cyclic voltammetry was tested. By contrast with the soluble initial OEPC, the thin film formed after cyclic voltammetry was insoluble in dichloromethane. This result is in agreement with the interchain coupling reaction (via pendant carbazole units) leading to a tridimensional structure. Moreover the UV-Visible characterization of the thin cross-linked film allows the evaluation of its optical band gap from the onset of the absorption band. The resulting value (3.24 eV after electrochemical coupling) is lower than that of the OEPC (3.42 eV) and confirms an increase of the electronic delocalization in agreement with the formation of biscarbazole units. The fluorescence characterization of the film before and after cross-linking also enlightens some differences. The initial OEPC film shows an emission band at 369 nm, while it is shifted at 410 nm after oxidizing coupling. Finally, thermal analyses of OEPC and cross-linked OEPC have been carried out. The starting OEPC oligomer exhibits a glass transition temperature at 76 °C, which increases up to 108 °C after electrochemical coupling in agreement with a stiffening of the macromolecular structure due to cross-linking.

The surface of spin-coated OEPC thin film has been studied by AFM (Fig. 5). Before cross-linking, the surface is quite smooth with a root-mean-square (RMS) roughness of around 0.23 nm. After cross-linking, large modifications of the surface morphology of the film are clearly seen; in particular, an increase of the surface roughness is observed. The RMS roughness is then about 2.3 nm. This evolution could be due to the incorporation of the electrolyte inside the tridimensional network during its formation.

Synthesis of semi-IPN

A *N*-methyl pyrrolidone solution of an OEPC and poly (Pery-EO_3) mixture (1/1 wt.%) was deposited on a platinum electrode, and subsequently evaporated. The modified electrode was then dipped into 0.1 M $LiClO_4$ in CH_3CN and the cross-linking of OEPC was carried out under cyclic voltammetry between −0.4 and 0.9 V vs Fc/Fc^+. The formation of the biscarbazole network in the presence of poly(Pery-EO_3) was observed, as already observed for the OEPC alone. Indeed, we observe during repeated scans the increase of the two biscarbazole redox systems, indicating the possible formation of semi-IPN.

In order to follow in real time the formation of the semi-IPN, and thus perform an indirect kinetic monitoring of this reaction, extraction experiments of the linear polyimide, i.e., poly(Pery-EO_3), from the biscarbazole-based network on the electrode have been performed in six independent experiments for increasing numbers of potential scans (0 to 10).

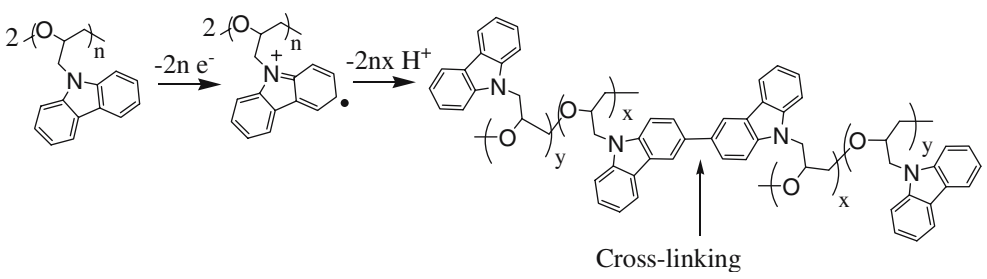

Fig. 4 Mechanism of electrochemical cross-linking of OEPC

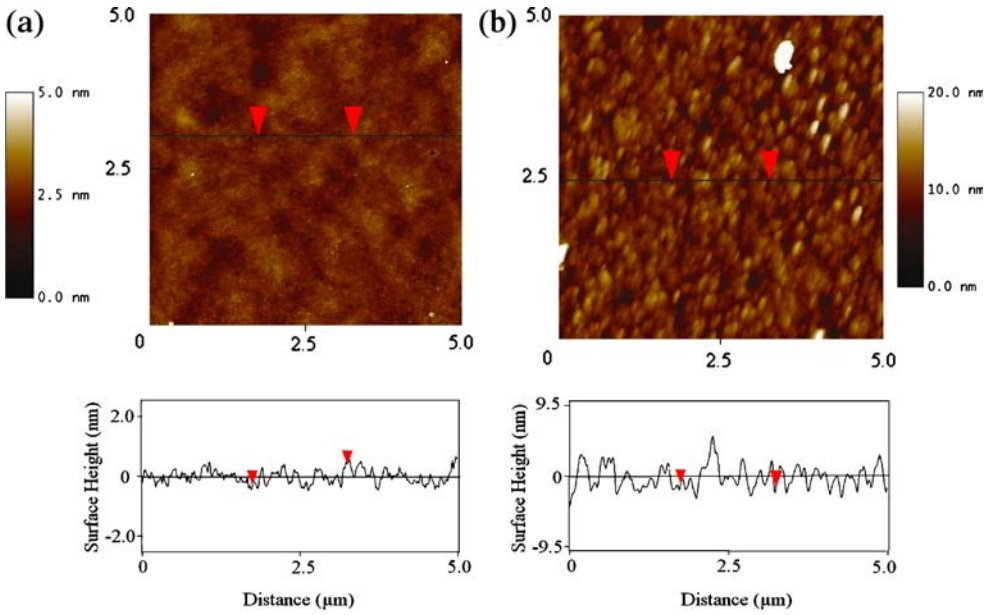

Fig. 5 AFM image of OEPC before and after potentiodynamic cross-linking

After electrochemical coupling of OEPC (at different scan potentials), each modified electrode is immersed for 1 min into *N*-methyl pyrolidone (NMP), which is a good solvent for poly(Pery-TEO). The UV-visible spectroscopy measurement of the absorbance of the resulting solution at 522 nm leads to the determination of the percentage of polyimide extracted from the film at the particular level of coupling, which arose during the given number of scans. Figure 6 shows the evolution of the percentage of poly(Pery-EO_3) dissolved in the NMP solution vs the number of potential scans performed resulting in cross-linking. Before cycling, the thin film is a mere blend of OEPC and poly(Pery-EO_3). In this case, which corresponds to the zero time of the semi-IPN formation reaction, all the polymers are solubilized after 1 min of immersion in NMP. By increasing the number of potential scan on a new starting mixture each time, we clearly observe a decrease of the extracted amount of the perylene derivative from the film. From ten cycles, corresponding probably to the full formation of the semi-IPN, only 4% of perylene dissolves into NMP. Such an evolution confirms that the formation of the biscarbazole network modifies the morphology of the film, which severely limits the rate of desorption of the perylene derivative towards the NMP.

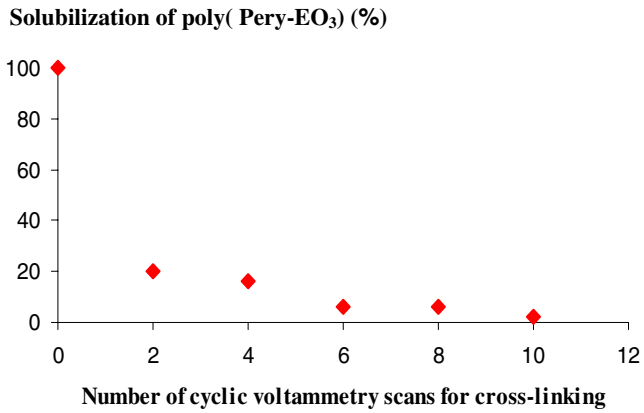

Fig. 6 Kinetics of extraction of poly(Pery-EO_3) during the formation of the biscarbazolyl network (by cyclic voltammetry)

Moreover, it is noticeable that the electroactivity of the biscarbazole network is quantitatively kept during the immersion in NMP while the macromonomer (without cross coupling) is soluble. It is a confirmation of the formation of the semi-IPN.

Electrochemical characterization and charge transfer properties

The electrochemical characterization of the semi-IPN was carried out by cyclic voltammetry in 0.1 M NBu_4ClO_4 in CH_3CN at different scan rates. Figure 7 reveals the simultaneous presence of the two oxidation peaks of biscarbazole group and the two reduction peaks of poly (Pery-EO_3), indicating that the two redox systems are electroactive inside the film. The semi-IPN behaves as an intrinsic p and n dopable material.

A linear relationship exists between the scan rate (v) and the peak current (I_p) of either the oxidation process of biscarbazole moieties or the reduction one of perylene units. This result seems to indicate a thin-layer electrochemical behavior. We are not in the configuration of a semi-infinite diffusion response corresponding to a Randles–Sevcik equation, in which peak current will be proportional to $v^{1/2}$.

The optical gaps $Eg_{optical}$ of the electron donor (biscarbazole network) and electron acceptor (perylene based polyimide) were determined from the onset of the absorption bands of each polymer deposited onto ITO. E_{HOMO} of

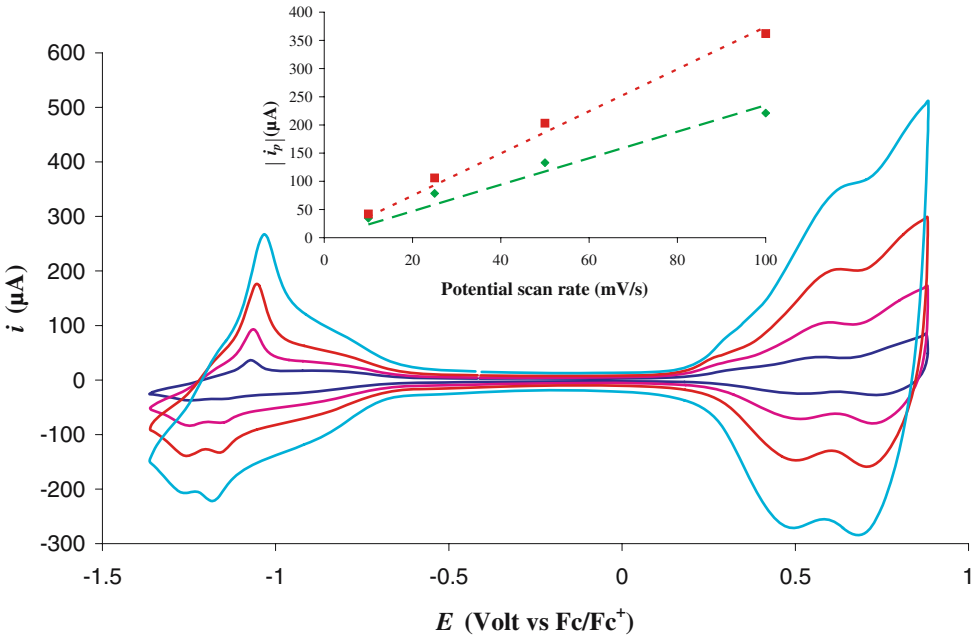

Fig. 7 Electrochemical characterization of the biscarbazole/perylene bisimide semi-IPN in CH_3CN/NBu_4ClO_4 (0.1 mol l^{-1}) at 10–25–50–100 mV s^{-1}. Evolution of the current peak vs potential scan rate (*insert*)

the biscarbazole network and E_{LUMO} of excited poly(Pery-EO_3) were estimated from the cyclic voltammetry by the onset of the oxidation and reduction of each redox unit, respectively [42]. E_{LUMO} of the biscarbazole network and E_{HOMO} of excited poly(Pery-EO_3) have been deduced from the optical band gap [43]. The corresponding values are gathered in Table 1.

In an aim to prepare photovoltaic devices using such semi-IPN, it can be assumed that perylene units will play the role of light harvesting (since the absorption of biscarbazyl is quite low in the visible range by comparison to the perylene absorption). The generation of excitons would mainly occur on perylene units and the higher energy of the HOMO of biscarbazyl units in the network should ensure the electron transfer to the HOMO of photoexcited perylene, as shown in Fig. 8.

The charge transfer process between the electron acceptor (perylene-based polymer) and the electron donor (carbazole derivative) can be confirmed following the evolution of the emission intensity of poly(Pery-EO_{34}) during the addition of a carbazole derivative. A *N*-butanesulfonate carbazole sodium salt ($CzSO_3Na$) (see "Experimental section") was chosen (Fig. 9) because the interactions of alkaline cation with ethyleneoxyde units should improve the interaction between the electron donor and the electron acceptor materials in dilute solution. Figure 9a shows that the presence of carbazole derivative quenches the emission of perylene derivative. The fluorescence quenching can be derived from the Stern–Volmer equation

$$I_O/I = 1 + K_{SV}[Q]$$

where I_o is the fluorescence intensity of poly(Pery-EO_{34}) without the addition of $CzSO_3Na$, I is the fluorescence intensity of poly(Pery-EO_{34}) upon the addition of $CzSO_3Na$, K_{SV} is the quenching constant, and $[Q]$ is the concentration of $CzSO_3Na$.

Figure 9b clearly shows the dependence of the relative fluorescence intensity I_O/I on the concentration of carbazole derivative. The value of the Stern–Volmer constant K_{SV} is 4.3 10^3 M^{-1}. By comparison, a similar experiment has been carried out using paratoluenesulfonate sodium salt in the same experimental conditions. In this case, no quenching of poly(Pery-EO_{34}) emission is observed, which confirms the contribution of carbazole units to the quenching possibly due to electron transfer from photoexcited perylene to carbazole moieties.

Table 1 Optical gap and energetic molecular orbital of biscarbazole network and poly(Pery-EO_3)

	$Eg_{optical}$[a] (eV)	E_{HOMO} (eV)	E_{LUMO} (eV)
Biscarbazole network	3.2	−5.1[b]	−1.9
Poly(Pery-EO_3)	1.8	−5.9	−4.1[b]

[a] Determined by UV-Vis spectra
[b] Determined by cyclic voltammetry

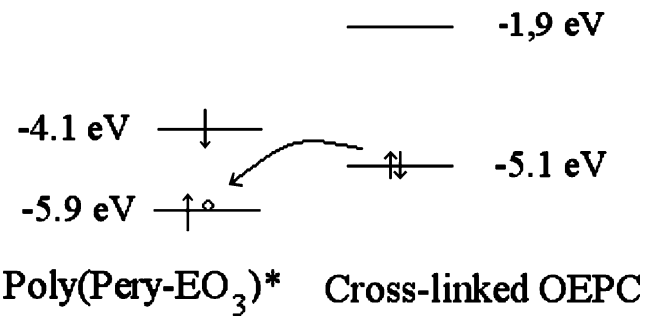

Fig. 8 Energetic diagram of cross-linked OEPC and excited poly (Pery-EO_3)

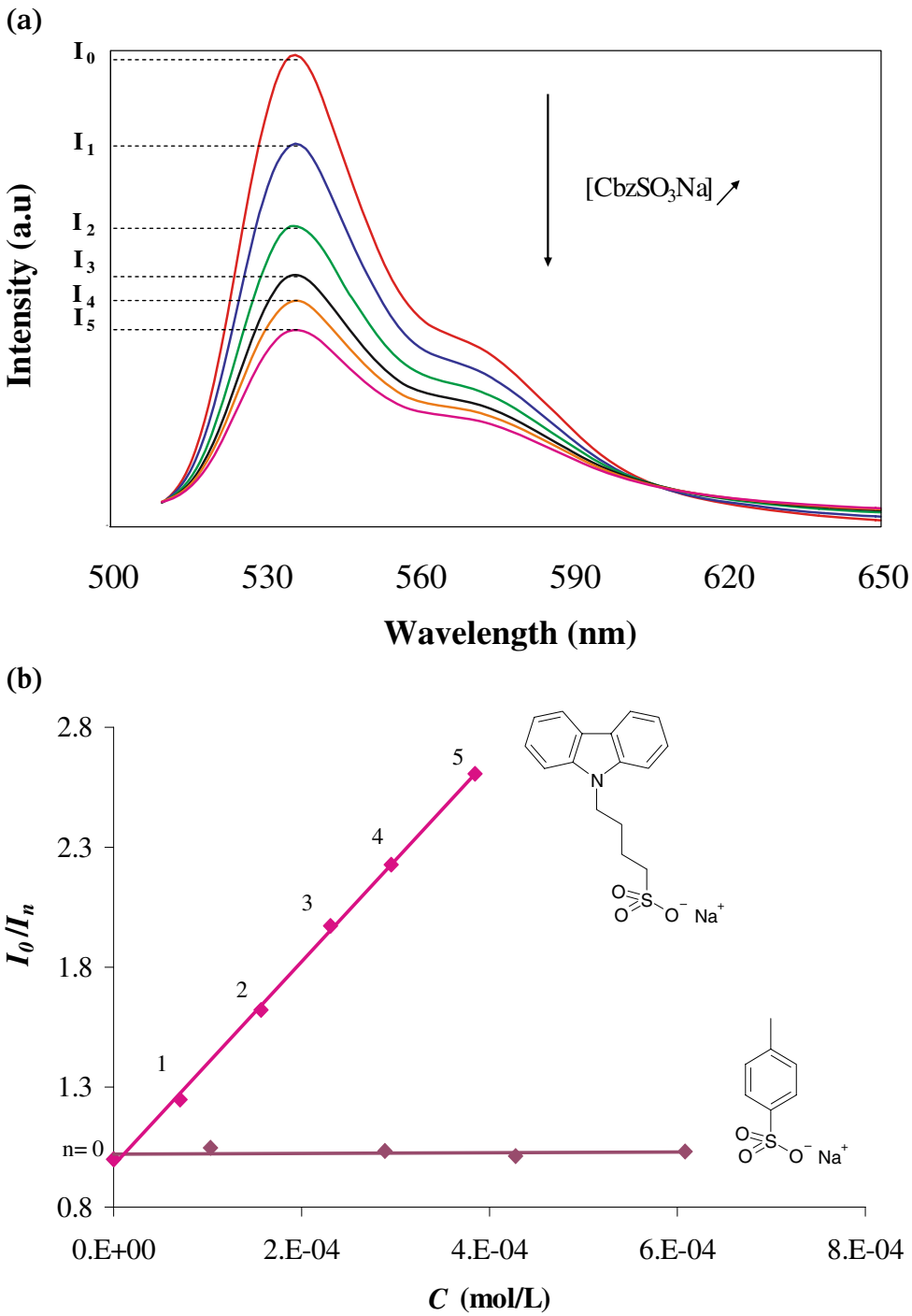

Fig. 9 **a** Evolution of the fluorescence intensity of poly(Pery-EO_{34}) (27 mg/l in water) after the addition of a *N*-butanesulfonatecarbazole sodium salt (0.7 10^{-4}, 1.6 10^{-4}, 2.3 10^{-4}, 3 10^{-4}, 3.8 10^{-4} mol l^{-1} λ_{ex}=537 nm. **b** Evolution of the relative emission intensity measured at 537 nm vs the concentration of *N*-butanesulfonatecarbazole sodium salt

Conclusions

This study describes the formation of an in-situ anodic cross-linking of a thin film from an oligomer bearing pendant carbazole groups. The charge transfer from the electrode to the film with concomitant incorporation of anions in the thin layer ensures the coupling of carbazole units in the bulk of the material, as confirmed by optical, thermal, and electrochemical characterizations.

The electrochemical cross-linking of a mixture of carbazole oligomer and perylene-based redox copolymer in the film leads to a semi-interpenetrating polymer network. Electroactivity determination of both biscarbazole and perylene redox units confirms the p and n dopable properties of the semi-IPN. An energetic diagram of the materials indicates the possibility to realize electron transfer between the electron donor and acceptor materials, as confirmed by preliminary results of fluorescence quenching of perylene bisimide materials by a carbazole derivative.

Acknowledgement Financial support from the joint French–Lithuanian research program "Gilibert" is gratefully acknowledged.

References

1. Yu G, Gao J, Hummelen JC, Wudl F, Heeger AJ (1995) Science 270:1789
2. Granström M, Petritsch K, Arias AC, Lux A, Andersson MR, Friend RH (1998) Nature 395:258
3. Sariciftci NS, Smilowitz L, Heeger AJ, Wudl F (1992) Science 258:1474
4. Halls JM, Walsh C, Groenham N, Marseglla E, Friend R, Maratti S, Holmes A (1995) Nature 376:498
5. Sariciftci NS (2004) Mater Today 7:36
6. Gebeyehu D, Bradec CJ, Padinger F, Fromherz T, Hummelen JC, Badt D, Schindler H, Sariciftci NS (2001) Synth Met 1: 118
7. Waldauf C, Schilinsky P, Hauch J, Brabec CJ (2004) Thin Solid Films 503:451
8. Kim Y, Cook S, Tuladhar SM, Choulis SA, Nelson J, Durrant JR, Bradley DDC, Giles M, McCulloch I, Ha CS, Ree M (2006) Nat Mater 5:197
9. Halls JJM, Friend RH (1997) Synth Met 85:1307
10. Tang CW (1986) Appl Phys Lett 48:183
11. Hua J, Meng F, Ding F, Li F, Tian H (2004) J Mater Chem 14:1849
12. Schmidt-Mende L, Fechtenkötter A, Mullen K, Moons E, Friends RH, MacKenie JD (2001) Science 293:1119
13. Tan L, Curtis MD, Francis AH (2003) Chem Mater 15:2272
14. Nakamura JI, Yokoe C, Murata K, Takahashi K (2004) J Appl Phys 96:6878
15. Burquel A, Lemaur V, Beljonne D, Lazzaroni R, Cornil J (2006) J Phys Chem A 110:3447
16. Onoda M, Tada K, Zakhidov AA, Yoshino K (1998) Thin Solid Films 331:76
17. Chochos CL, Govaris GK, Kakali F, Yiannoulis P, Kallitsis JK, Gregoriou VG (2005) Polymer 46:4654
18. Kymakis E, Amaratunga GAJ (2002) Appl Phys Lett 80:112
19. Rahman GMA, Guldi DM, Cagnoli R, Mucci A, Schenetti L, Vaccari L, Prato M (2005) J Am Chem Soc 12:10051
20. Horowitz G, Kouki F, Spearman P, Fichou D, Nogues C, Pan X, Garnier F (1996) Adv Mater 8:242
21. Ranke P, Bleyl I, Simmerer J, Haarer D, Bacher A, Schmidt HW (1997) Appl Phys Lett 71:1332
22. Perrec V, Glodde M, Bera TK et al (2002) Nature 419:384
23. Struijk CW, Sieval AB, Dakhorst JEJ, Dijk MV, Kimkes P, Koehorst RBM, Donker H, Schaafsma TJ, Picken SJ, Van de Craats AM, Warman JM, Zuilhof H, Sudhölter EJR (2000) J Am Chem Soc 122:11057
24. Bernede JC, Derouiche H, Djara V (2005) Sol Energy Mater Sol Cells 87:261
25. Nobuyuki I, Tsutomu M (2005) Chem Commun 14:1886
26. Shi MM, Chen HZ, Sun JZ, Ye J, Wang M (2003) Chem Phys Lett 381:666
27. Chen HZ, Shi MM, Aernouts T, Wang M, Borghs G, Heremans P (2005) Sol Energy Mater Sol Cells 87:521
28. Li J, Dierschke F, Wu J, Grimsdale AC, Müllen K (2006) J Mater Chem 16:96
29. Grazulevicius JV, Strohriegl P, Pielichowski J, Pielichowski K (2003) Prog Polym Sci 28:1297
30. Michot C, Baril D, Armand M (1995) Sol Energy Mater Sol Cells 39:289
31. Williams ME, Murray RW (1998) Chem Mater 10:3603
32. Buika G, Grazulevicius JV (1993) Eur Polym J 29:1489
33. Reynolds JR, Qiu YJ (1990) J Electrochem Soc 137:900
34. Ko HC, Lim DK, Choi W, Lee H (2004) Synth Met 144:177
35. Neuteboom EE, Janssen RAJ, Meijer EW (2001) Synth Met 121:1283
36. Wang W, Han JJ, Wang LQ, Li LS, Shaw WJ, Li ADQ (2003) Nano Lett 3:455
37. Gregg BA, Cormer RA (1998) J Phys Chem B 102:9952
38. Lu W, Gao JP, Wang ZY, Qi Y, Sacripante GG, Duff JD, Sundararajan PR (1999) Macromolecules 32:8880
39. Ambrose JF, Nelson RF (1968) J Electrochem Soc 115:1159
40. Ambrose JF, Carpenter LL, Nelson RF (1975) J Electrochem Soc 122:876
41. Armand M, Chabagnot JM, Duclot M (1979) In: Vahista P, Mundy JN, Shenoy GK (eds) Fast ion transport in solids. North-Holland, Amsterdam, p 131
42. Cervini R, Li XC, Spencer GWC, Holmes AB, Moratti SC, Friend RH (1997) Synth Met 84:359
43. Shin WS, Jeong HH, Kim MK, Jin SH, Kim MR, Lee JK, Lee JW, Gal YS (2006) J Mater Chem 16:384